



ACADEMIC  
PRESS

Available online at [www.sciencedirect.com](http://www.sciencedirect.com)

SCIENCE @ DIRECT®

Journal of Sound and Vibration 262 (2003) 161–173

---

---

JOURNAL OF  
SOUND AND  
VIBRATION

---

---

[www.elsevier.com/locate/jsvi](http://www.elsevier.com/locate/jsvi)

# Force identification by means of in-operation modal models

E. Parloo\*, P. Verboven, P. Guillaume, M. Van Overmeire

*Department of Mechanical Engineering, Vrije Universiteit Brussel, TW-WERK, Pleinlaan 2, B-1050 Brussels, Belgium*

Received 26 November 2001; accepted 27 March 2002

---

## Abstract

In-operation modal analysis has become a valid alternative for structures where a classic forced-vibration test would be difficult if not impossible to conduct. The modelling of output-only data obtained from naturally excited structures is particularly interesting because the test structure remains in its normal in-operation condition during the test. One of the drawbacks of in-operation analysis is that part of the modal parameters can no longer be estimated. Consequently, the applicability of in-operation modal models remains somewhat restricted. For some in-operation applications, interest lies in the identification of the forces that gave rise to the measured response signals. In order to solve this ill-conditioned problem, a complete modal model of the structure is required. Recently, a sensitivity-based method was proposed for the normalization of operational mode shape estimates on the basis of in-operation modal models only. This method allows the reconstruction of complete modal models from output-only data. In this paper, the possibility of using such re-completed in-operation modal models for the identification of localized forces is explored.

© 2002 Elsevier Science Ltd. All rights reserved.

---

## 1. Introduction

In the past few years, the identification of output-only data has received a considerable amount of attention. Adapting model-based system identification techniques (e.g., maximum likelihood estimator, least-squares complex exponential estimator, subspace techniques) for use with output-only data, has created the possibility of estimating modal models for in-operation structures excited by ambient noise and vibration (e.g., traffic, wind, waves, etc.) [1–3]. For some structures, in-operation modal analysis is the only way of obtaining an experimental modal model since classic forced-vibration tests are sometimes difficult or impossible to conduct, at least with standard testing material. Moreover, the use of artificial excitation devices (shakers, drop weights) is considered expensive and unpractical especially in cases where the ambient excitation sources

---

\*Corresponding author. Tel: +32-2-629-2807; fax: +32-2-629-2865.

*E-mail address:* [Eli.Parloo@vub.ac.be](mailto:Eli.Parloo@vub.ac.be) (E. Parloo).

cannot be excluded from the measurement set-up (e.g., civil structures). The modelling of output-only data obtained from naturally excited structures is particularly interesting because the test structure remains in its normal in-operation condition during the test. This can be considered as an advantage, since the condition of the test structure during a laboratory forced-vibration test often differs significantly from the structure's real in-operation working conditions. An example is given by high-speed ships where the mass loading of water adjacent to the hull varies with the speed of the ship through the water. Since changes in mass loading induce changes in modal parameters, the dynamic behaviour of the ship will depend upon its speed. Other vehicles or structures (e.g., bridges open for traffic, offshore platforms, cars, trains, etc.) show a similar response to changes in working condition [4–8]. For some in-operation applications, interest lies in the identification of the forces that gave rise to a given (measured) set of response signals. For this purpose, a complete modal model is required. One of the drawbacks of operational analysis is that part of the modal parameters can no longer be estimated. Since the ambient forces that excite the test structure are not being measured, the modal participation factors can no longer be determined. Consequently, the estimated operational mode shapes are not correctly scaled since their scaling factor will depend on the unknown ambient excitation. So far, techniques are not available for the normalization of operational mode shapes purely on the basis of output-only data. All known methods either involve a detailed knowledge of the material characteristics of the test structure (finite element model approach [9]) or make very restrictive assumptions about the excitation [10]. Another method involves performing an additional forced vibration test, in a limited number of points, in order to re-scale the in-operational mode shape estimates [11]. Recently, a novel approach was presented for the normalization of operational mode shapes on a basis of in-operation modal models only [12]. It is shown that by adding or removing, for instance, one (or more) masses (with well-known weights) to the test structure, the operational mode shapes can be normalized by means of the measured shift in natural frequencies between the original and mass-loaded condition. By normalizing the operational mode shapes, a complete modal model can be reconstructed. On the basis of this model, an inverse problem can be formulated for the identification of the unknown forces that gave rise to the measured responses. In Ref. [13], the force identification problem was addressed and an inverse solver was proposed and compared to classic approaches (e.g., pseudo-inverse). In this paper, the proposed inverse solver was evaluated in combination with the sensitivity-based normalization approach. Previously, the sensitivity-based normalization technique was successfully used in a similar inverse problem, namely, the identification of damage from output-only data [14]. Initially, the in-operation modal models are re-completed by means of the sensitivity-based normalization approach. Second, the inverse solver proposed in Ref. [13] is used for the identification of the force(s). The approach is validated by means of experiments performed on a beam structure.

## **2. Theoretical aspects**

### *2.1. Introduction*

The following sections give a theoretical overview of the followed approach. The computation of modal parameter sensitivity and the sensitivity-based normalization technique are briefly

discussed in Sections 2.2 and 2.3. The identification of forces from the complete modal models is treated in Section 2.4.

## 2.2. Sensitivity of modal parameters

The technique proposed in Ref. [12], for the normalization of mode shape estimates obtained from operational data, is based on the use of modal parameter sensitivity to local changes in mass. As shown in the literature [15], the sensitivity of modal parameters to local changes in mass, stiffness or damping can be calculated by means of the estimated poles and normalized mode shapes without the use of a finite element model (FEM). As an example, the sensitivity of degree of freedom (d.o.f.)  $j$  of a mass-normalized mode shape  $i$  to a local change in mass at d.o.f.  $k$  is given by

$$\frac{\partial \phi_{ji}}{\partial m_k} \approx -\frac{\phi_{ki}^2}{2} \phi_{ji} + \phi_{ki} \sum_{r=1, r \neq i}^{N_m} \frac{\omega_r^2}{(\omega_r^2 - \omega_i^2)} \phi_{kr} \phi_{jr} \quad (1)$$

with  $N_m$  being the number of modes, whereas the sensitivity of natural frequency  $\omega_i$  to a local change in mass in d.o.f.  $k$  is given by

$$\frac{\partial \omega_i}{\partial m_k} = -\omega_i \frac{\phi_{ki}^2}{2}. \quad (2)$$

For an undamped system, Eq. (1) is exact if all  $N_m$  modes of the structure are taken into account. Despite the fact that only a limited number of modes can be determined experimentally in general, a good approximation of the mode shape sensitivity can be obtained. It is important to note that for the calculation of the sensitivity of the natural frequency in Eq. (2), only the corresponding mode shape vector is required. Hence, the sensitivity of the natural frequencies will be more exact. Similar expressions can be written for the sensitivity of modal parameters to local changes in stiffness [15,16]. Moreover, damping can be taken into account by assuming a general viscous damped system. For real-life engineering structures with little damping present (normal mode shapes) and a predominant linear behaviour, Eqs. (1) and (2) usually form a good approximation for the sensitivity of the estimated natural frequencies and mode shapes.

Sensitivity analysis has proven to be extremely useful in several application domains. A first example is given by the (re)design of prototypes. A sensitivity analysis is a fast and easy method to use to predict the effect of modifications on the dynamics of a prototype without having to apply any actual high-cost changes to the structure [15,17]. An example is the use of modal parameter sensitivity for the compensation of mass loading effects induced by transducers and accelerometers [16–19]. By solving an inverse problem, a sensitivity analysis can also be used for the localization and assessment of structural damage [14,20]. In the following section, a sensitivity-based method will be introduced for the normalization of operational mode shape estimates.

## 2.3. Sensitivity-based normalization of operational mode shapes

In Refs. [12,14], a sensitivity-based method was presented for the normalization of operational mode shape estimates obtained from output-only vibration data. Eqs. (1) and (2) require the use

of correctly normalized mode shape estimates. In the case of a classical forced-vibration test, where the input forces are measured, a full modal model of the structure can be determined. As long as a driving-point measurement is performed, the mode shape estimates obtained can be scaled according to any normalization scheme desired [15]. During an in-operational modal analysis, only part of the modal model can be determined. Since the ambient forces that excite the structure are no longer being measured, the modal participation factors cannot be determined. As a result, the estimated mode shape vectors remain unscaled (i.e., dependant on the unknown level of ambient excitation) [21]. The relationship between the unscaled ( $N_o \times 1$ ) mode shape vector  $\{\Psi\}_i$  (as obtained by in-operation modal analysis) and the corresponding correctly normalized mode shape vector  $\{\Phi\}_i$ , obtained from a classical forced-vibration test, of mode  $i$  can therefore be expressed by

$$\{\Phi\}_i = \alpha_i \{\Psi\}_i \quad (3)$$

with  $\alpha_i$  being an operational scaling factor for mode  $i$  dependant on the level of ambient excitation and  $N_o$  the number of outputs. It is shown in Ref. [12] that an estimate of the operational scaling factor can be obtained by performing a controlled mass addition experiment on the test structure. A first order approximation of  $\alpha_i$  for a normal mode  $i$  is given by

$$\alpha_i \simeq \sqrt{-\frac{2\Delta\omega_i}{\omega_i \sum_{k=1}^N (\psi_{ki})^2 \Delta m_k}} \quad (4)$$

with  $k$  being the position of mass change  $\Delta m_k$  and  $N$  the number of mass changes used. The addition or removal of a small known mass  $\Delta m_k$ , in d.o.f.  $k$  of the test structure, will induce a change in natural frequencies between the original and the mass-loaded condition. The experimental determination of this change  $\Delta\omega_i$ , together with the in-operational modal model of the original structure, is sufficient to provide an estimate of the operational scaling factor  $\alpha_i$ . It should be noted that the change in natural frequency  $\Delta\omega_i$  can be experimentally obtained from a single measurement in a well-chosen point of the structure. Placing the mass in or near a nodal point of the mode shape vector considered for re-scaling should be avoided. The change in the corresponding poles of the mass-loaded and the original condition will be very small. Using such a location might produce incorrect scaling results due to the presence of uncertainties on the estimated poles.

#### 2.4. Source identification

Once the operational mode shape estimates are normalized, the frequency response functions (FRFs)  $H_{oi}(\omega)$  between output  $o$  and input  $i$  can be synthesized for all frequencies  $\omega$  in the considered bandwidth by

$$H_{oi}(\omega) = \sum_{r=1}^{N_m} \left( \frac{Q_r \phi_{or} \phi_{ir}}{(j\omega - \lambda_r)} + \frac{Q_r^* \phi_{or}^* \phi_{ir}^*}{(j\omega - \lambda_r^*)} \right) \quad (5)$$

with  $\lambda_r$  being the pole of mode  $r$  and  $Q_r$  a modal scaling factor dependent on the type of normalization (e.g.,  $Q_r = 1/(2j\omega_r)$  for mass normalization). The complex conjugate is hereby denoted as  $(\cdot)^*$ . On a basis of these FRFs, the following input–output relation can be written as

$$\{\mathbf{X}(\omega_f)\} = [\mathbf{H}(\omega_f)]\{\mathbf{F}(\omega_f)\} \quad (6)$$

with  $[\mathbf{H}(\omega_f)]$  being the  $(N_o \times N_o)$  FRF matrix,  $\{\mathbf{X}(\omega_f)\}$  and  $\{\mathbf{F}(\omega_f)\}$  the  $(N_o \times 1)$  column vectors with, respectively, the spectra of the responses and forces. By solving the inverse problem

$$\{\mathbf{F}(\omega_f)\} = [\mathbf{H}(\omega_f)]^{-1} \{\mathbf{X}(\omega_f)\}, \quad (7)$$

the unknown forces can be identified on the basis of the measured response spectra for all  $N_f$  frequencies  $\omega_f$  of the considered frequency band. In Ref. [13], an algorithm is presented to estimate, starting from the measured response spectra and the estimated modal model, the forces that are acting on a structure. Force identification requires the inversion of FRF matrices, which are derived from the estimated modal model. These FRF matrices are, however, badly conditioned due to rank deficiency. In practice, a pseudo-inverse of the FRF matrix is often used [22],

$$\{\mathbf{F}(\omega_f)\} = [\mathbf{H}(\omega_f)]^+ \{\mathbf{X}(\omega_f)\}. \quad (8)$$

This approach results in forces that are distributed over the whole structure. This means that it is not always straightforward to detect the position of the sources. A better localization is possible by using an iterative ‘weighted’ pseudo-inverse defined as

$$\{\mathbf{F}(\omega_f, \mathbf{W})\} = [\mathbf{W}][[\mathbf{H}(\omega_f)][\mathbf{W}]]^+ \{\mathbf{X}(\omega_f)\} \quad (9)$$

with  $[\mathbf{W}] = \text{diag}(\{w_1, w_2, \dots\})$  a (frequency-independent) diagonal weighting matrix. If  $[\mathbf{H}(\omega_f)][\mathbf{W}]$  is of full rank, Eq. (9) reduces to the classic pseudo-inverse solution. This can be easily seen by right multiplying both sides of Eq. (8) with  $[\mathbf{W}]^+$  and recalling that  $([\mathbf{H}(\omega_f)][\mathbf{W}])^+ = [\mathbf{W}]^+[\mathbf{H}(\omega_f)]^+$  when both matrices are of full rank. In that case, the weighting matrix  $[\mathbf{W}]$  has no influence on the identified forces. However, if  $[\mathbf{H}(\omega_f)][\mathbf{W}]$  is rank deficient, then all singular values smaller than a given tolerance are neglected during the computation of the pseudo-inverse. Consequently, Eq. (9) no longer equals a classic pseudo-inverse because the resulting force vector  $\{\mathbf{F}(\omega_f, \mathbf{W})\}$  will depend on the weighting matrix  $[\mathbf{W}]$ . This matrix right multiplies the FRF matrix allowing to put more emphasis (or weight) on some input locations while other locations—corresponding with zero or small  $w$ -values—are eliminated. Because  $[\mathbf{H}(\omega_f)]$  is rank deficient, it is not possible to find a unique solution for the force since an infinite amount of solutions exists. By using a weighted pseudo-inverse, an infinite set of force vectors  $\{\mathbf{F}(\omega_f, \mathbf{W})\}$ , dependant on  $[\mathbf{W}]$ , are obtained. All these possible solutions satisfy the input–output relation (6) since

$$[\mathbf{H}(\omega_f)]\{\mathbf{F}(\omega_f)\} = [\mathbf{H}(\omega_f)][\mathbf{W}][[\mathbf{H}(\omega_f)][\mathbf{W}]]^+ \{\mathbf{X}(\omega_f)\} = \{\mathbf{X}(\omega_f)\}. \quad (10)$$

The diagonal weighting matrix  $[\mathbf{W}] = \text{diag}(\{\mathbf{w}\})$  (with  $\{\mathbf{w}\} = \{w_1, w_2, \dots\}$ ) is determined in such a way that the  $\ell_p$ -norm of the forces is minimized.

$$K(\mathbf{W}) = \sum_{f=1}^{N_f} \|\{\mathbf{F}(\omega_f, \mathbf{W})\}\|_p^p \quad (11)$$

with  $p$  being a value close to zero (e.g., 0.01) and  $\|\{\mathbf{F}\}\|_p^p = (1/N_o) \sum_{i=1}^{N_o} |F_i|^p$ . Note that for  $p \rightarrow 0$ , the  $\ell_p$ -norm  $\|\{\mathbf{F}(\omega_f, \mathbf{W})\}\|_p^p$  converges to the number of entries in  $\{\mathbf{F}(\omega_f, \mathbf{W})\}$  different from zero. Hence, minimizing Eq. (11) corresponds to making as many entries as possible of  $\{\mathbf{F}(\omega_f, \mathbf{W})\}$  equal to zero, i.e., finding the solution requiring the lowest possible amount of locations.

Because the  $\ell_p$ -norm is differentiable with respect to  $[\mathbf{W}]$ , cost function (11) can be minimized by means of classical optimization algorithms. Note that Eq. (11) can be written as

a quadratic cost function

$$K(\mathbf{W}) = \frac{1}{N_o} \sum_{f=1}^{N_f} \sum_{i=1}^{N_o} |R_i(\omega_f, \mathbf{W})|^2 \quad (12)$$

with

$$R_i(\omega_f, \mathbf{W}) = |F_i(\omega_f, \mathbf{W})|^{p/2}. \quad (13)$$

This quadratic cost function can be minimized using the Gauss–Newton optimization algorithm. An analytical expression for the Jacobian matrix  $[\mathbf{J}] = \partial\{\mathbf{R}\}/\partial\{\mathbf{w}\}$ , i.e., the derivative of the residue (13) with respect to  $[\mathbf{W}] = \text{diag}(\{\mathbf{w}\})$ , can be obtained. One can verify that the entries  $[\mathbf{J}]_{ij} = \partial R_i / \partial w_j$  of the Jacobian matrix equal

$$\frac{\partial R_i}{\partial w_j} = \frac{p}{2} |F_i|^{p/2-2} \left( \text{Re}(F_i) \text{Re} \left( \frac{\partial F_i}{\partial w_j} \right) + \text{Im}(F_i) \text{Im} \left( \frac{\partial F_i}{\partial w_j} \right) \right) \quad (14)$$

with  $\text{Re}(\cdot)$  and  $\text{Im}(\cdot)$ , respectively, denoting the real and the imaginary part. The derivatives  $\partial F_i / \partial w_j = [\partial\{\mathbf{F}\} / \partial\{\mathbf{w}\}]_{ij}$  are given by

$$\frac{\partial\{\mathbf{F}\}}{\partial\{\mathbf{w}\}} = ([\mathbf{I}] - [\mathbf{W}][[\mathbf{H}][\mathbf{W}]^+[\mathbf{H}]])[\mathbf{W}]^+[\mathbf{F}] \quad (15)$$

with  $[\mathbf{F}] = \text{diag}(\{\mathbf{F}\})$  and  $[\mathbf{W}] = \text{diag}(\{\mathbf{w}\})$ . Thanks to the fact that the Jacobian matrix can be computed analytically using Eqs. (14) and (15) (instead of using time-consuming finite difference approximations), a significant reduction of the computation time is obtained [13].

For an objective localization of the force(s), force indices can be calculated for each d.o.f.  $k$  of the structure on a basis of the identified force vector

$$\beta_k = \frac{\sum_{f=1}^{N_f} |\{F_k(\omega_f)\}|^2}{\sum_{k=1}^{N_o} \sum_{f=1}^{N_f} |\{F_k(\omega_f)\}|^2}. \quad (16)$$

If a localized force is present at d.o.f.  $k$ , a high value for the force index at that location will be obtained.

### 3. Experimental results

In order to illustrate the effectiveness of the combined approach of the sensitivity-based normalization technique [12] and the inverse solver proposed in Ref. [13], the following experiments were performed. A 1 kg steel beam (0.840 m  $\times$  0.030 m  $\times$  0.005 m) was elastically suspended in free–free conditions. An input–output experimental set-up was constructed in order to allow a full evaluation of the results from the proposed force identification techniques. Vibration response measurements were performed by means of a scanning laser vibrometer in 55 collinear locations along the full length of the beam. Throughout the experiments, the beam was excited with a stationary multi-sine signal by means of an electromechanical shaker positioned in d.o.f. 55 (at one end of the structure). The applied stationary force was measured simultaneously with each response measurement by means of a force cell. A maximum likelihood (ML) estimator [23] was used for the estimation of the modal parameters of the first six bending modes of the

beam. Since input–output measurements were performed, the mode shape estimates could be easily (mass-)normalized by means of a driving point measurement in d.o.f. 55. In case of in-operation modal data, a different approach is required since a driving point measurement is not available. For this reason, a second independent mass normalization of the reference condition was performed by means of a controlled mass change experiment. For this purpose, a small mass (weighing  $10.95 \times 10^{-3}$  kg) was removed from d.o.f. 1 of the structure. The experimental determination of the induced shift in natural frequency allows the estimation of operational scaling factors from Eq. (4) for each of the considered modes. An overview of the results can be found in Table 1. These include the natural frequency  $\omega_i$  and damping ratio  $\xi_i$  of the reference condition together with the shift in natural frequency  $\Delta\omega_i$  induced by the mass change in d.o.f. 1 for each mode  $i$  ( $i = 1, \dots, 6$ ). A comparison between the first set of mass-normalized mode shapes ‘ $\circ$ ’, scaled by means of the driving point measurement, and the second set ‘ $\times$ ’, scaled by means of the described mass addition experiment, is presented in Fig. 1 for the first four modes. It can be clearly seen that the results of the sensitivity-based method are in good agreement with those of the driving point mass normalization. This fact can be observed more quantitatively by calculating the modal scaling factors (MSF) between the first and second set of mass-normalized mode shapes. As can be seen from Table 1, these values are close to unity indicating a good agreement between both normalization methods. A more thorough validation of the sensitivity-based normalization technique, based on the comparison of forced response and in-operation modal data, can be found in Ref. [12].

Once the ‘operational’ mode shape estimates are normalized according to the sensitivity-based technique, a full modal model can be reconstructed according to Eq. (5). For the experiments on the beam, a  $(55 \times 55)$  FRF matrix can be calculated for every considered frequency. As an example of the quality of the reconstruction, Fig. 2 shows the amplitudes and phases of the measured ‘+’ and synthesized ‘-’ FRF between input 55 and output 55 (driving point location). A good correspondence between the measured and synthesized FRF can be observed. Similar results can be obtained in case a driving-point normalization was used for the reconstruction of the FRF data set.

On the basis of the synthesized FRFs, an inverse problem can be formulated for the identification of the ‘unknown’ forces (see Section 2.4). By solving the inverse problem and calculating the normalized force indices, information can be obtained on the location of the force(s). Figs. 3–4 show the results for the force indices obtained respectively, with the

Table 1  
Overview of the sensitivity-based normalization results

| Mode | $\omega_i$ (rad/s) | $\xi_i$ (%) | $\Delta\omega_i$ (rad/s) | MSF   |
|------|--------------------|-------------|--------------------------|-------|
| 1    | 282.76             | 0.023       | 4.82                     | 1.037 |
| 2    | 768.16             | 0.061       | 12.02                    | 1.032 |
| 3    | 1499.87            | 0.027       | 21.71                    | 1.024 |
| 4    | 2466.78            | 0.017       | 33.61                    | 0.988 |
| 5    | 3652.09            | 0.030       | 48.27                    | 1.005 |
| 6    | 5028.36            | 0.097       | 64.00                    | 0.812 |

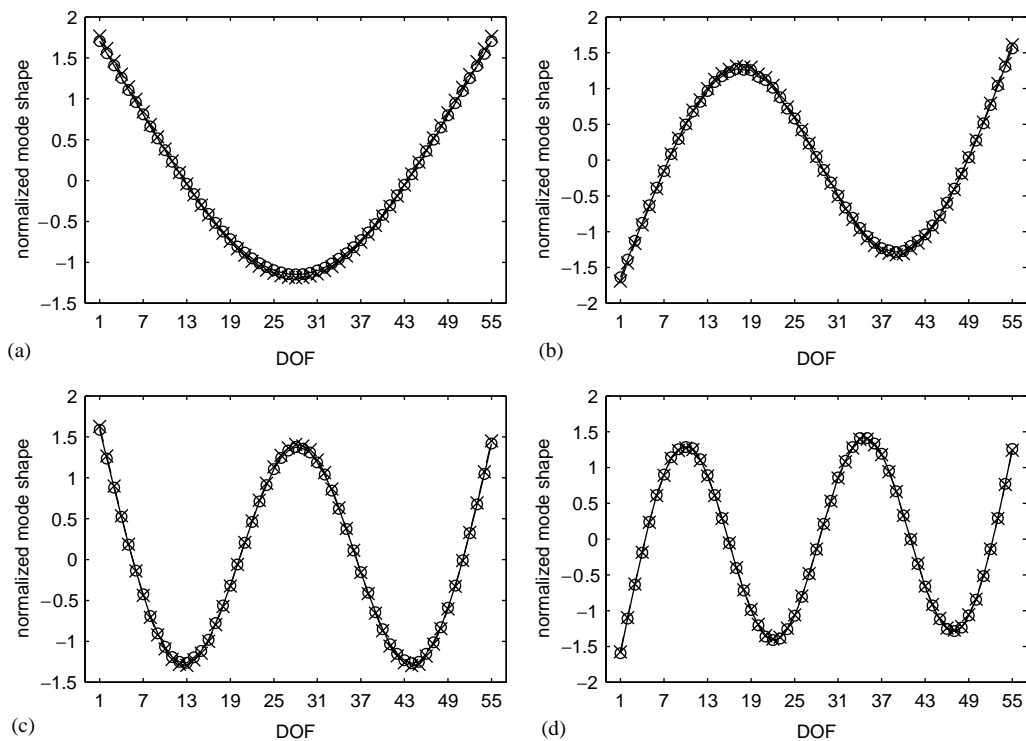


Fig. 1. Comparison of mode shape normalization results for the first four bending modes: driving point ‘o’ and sensitivity-based ‘x’ normalization results.

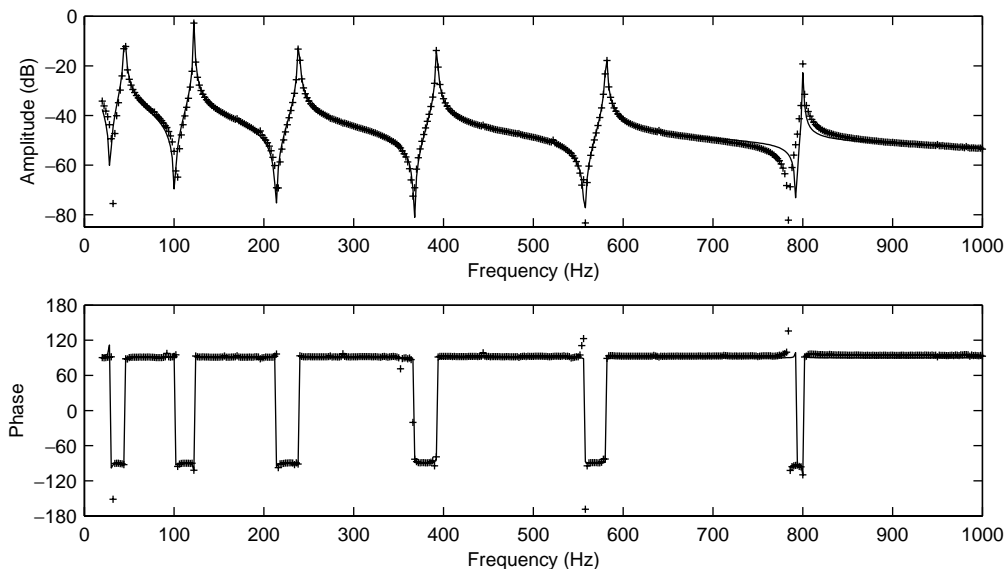


Fig. 2. Measured ‘+’ and synthesized ‘-’ FRF for driving-point location.



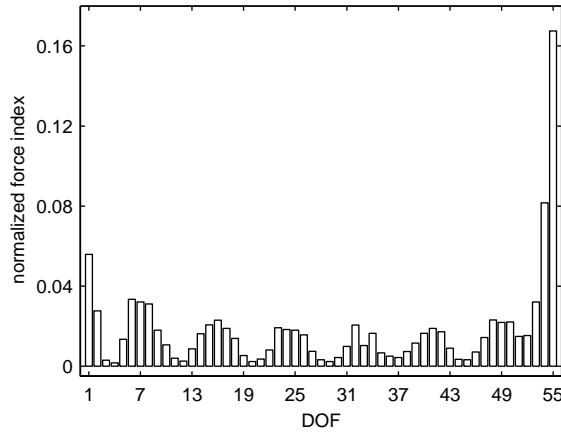


Fig. 3. Force localization result on the basis of pseudo-inverse and the sensitivity-based FRFs.

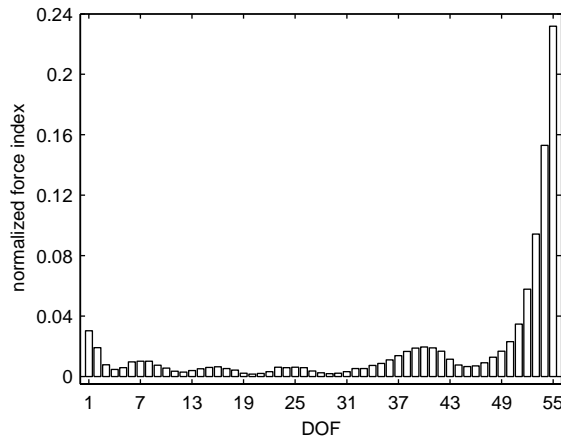


Fig. 4. Force localization result on the basis of pseudo-inverse and the driving-point FRFs.

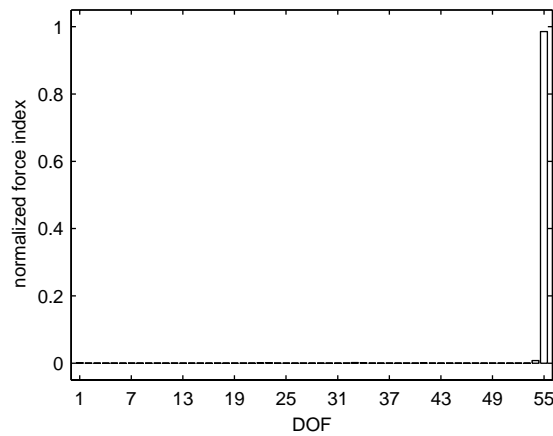


Fig. 5. Force localization result on the basis of weighted pseudo-inverse and the sensitivity-based FRFs.

sensitivity-based FRF data set and the driving point FRF data set. In both cases, a classic pseudo-inverse approach was used for solving the inverse problem. Both plots show a high force index for d.o.f. 55, revealing the actual force location for both data sets. However, it should be noted that the results do not exclude the presence of smaller forces in other locations. If the proposed iterative weighted pseudo-inverse is used for the identification of the force(s), the force localization results improve dramatically (Figs. 5 and 6). As before, the correct force location is

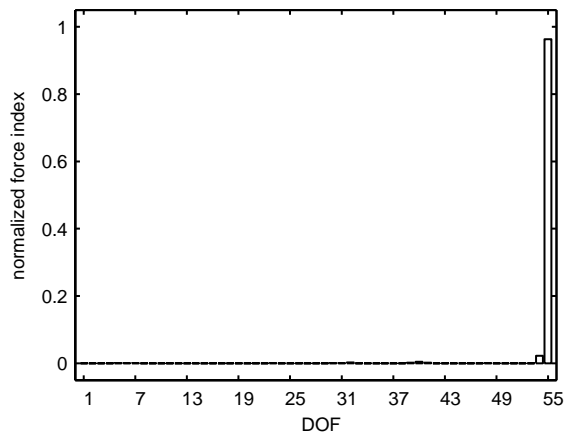


Fig. 6. Force localization result on the basis of weighted pseudo-inverse and the driving-point FRFs.

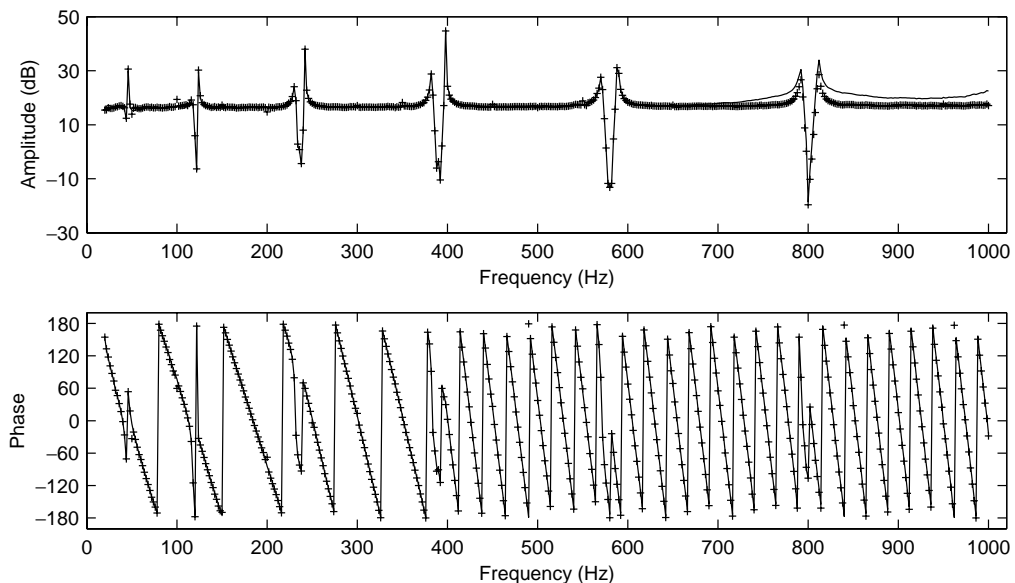


Fig. 7. Comparison between synthesized and measured force based on the sensitivity-based FRFs.

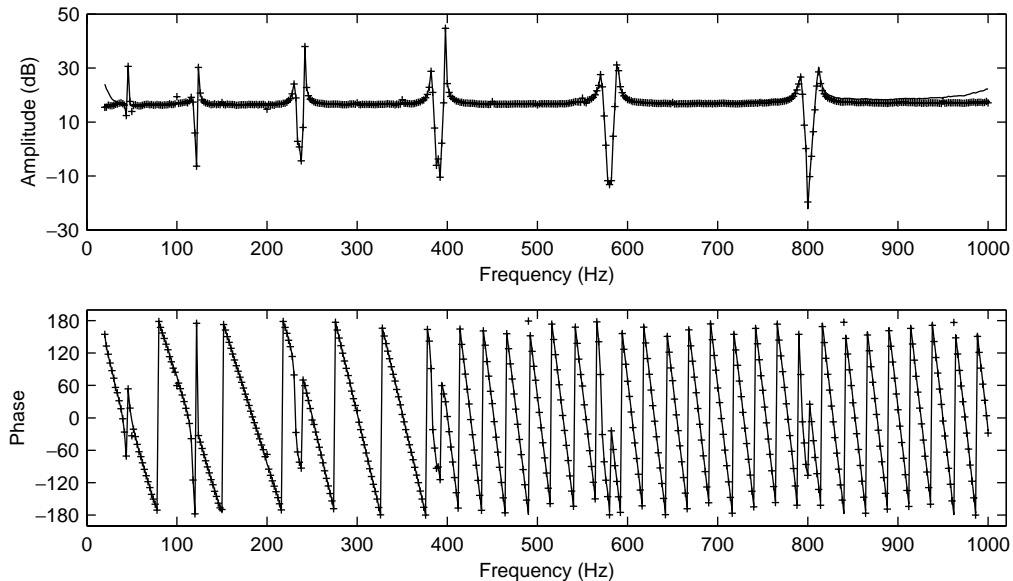


Fig. 8. Comparison between synthesized and measured force based on the driving-point FRFs.

identified for both data sets. Moreover, the results (almost) exclude the presence of forces in other locations.

Once the correct force location(s) are revealed, the actual force(s) (amplitude and phase) can be identified in the considered frequency range by means of a simple pseudo-inverse. Figs. 7 and 8 show the amplitudes and phases for the measured '+' and identified '-' force spectrum in d.o.f. 55 for both FRF data sets. Once again, good correspondence is observed for both magnitude and phases.

#### 4. Conclusions

In this paper, the applicability of the sensitivity-based normalization approach for force identification on the basis of output-only data was successfully evaluated. The quality of the reconstructed FRF data and the advantages of using an iterative weighted pseudo-inverse over a classic pseudo-inverse were illustrated by means of experiments performed on a beam structure.

#### Acknowledgements

This research has been supported by the Fund for Scientific Research—Flanders (Belgium) (FWO), the Institute for the Promotion of Innovation by Science and Technology in Flanders (IWT) and by the Research Council (OZR) of the Vrije Universiteit Brussel (VUB).

## References

- [1] L. Hermans, H. Van der Auweraer, M. Abdelghani, Critical evaluation of modal parameter extraction schemes for output-only data, *Proceedings of the International Modal Analysis Conference Japan (JMAC)*, 1997, pp. 682–688.
- [2] L. Hermans, H. Van der Auweraer, P. Guillaume. A frequency-domain maximum likelihood approach for the extraction of modal parameters from output-only data. *Proceedings of the 23rd International Seminar on Modal Analysis (ISMA23)*, September 1998, pp. 367–376.
- [3] P. Guillaume, L. Hermans, H. Van der Auweraer, Maximum likelihood identification of modal parameters from operational data. *Proceedings of the 17th International Modal Analysis Conference (IMAC17)*, February 1999, pp. 1887–1893.
- [4] O. Loland, J.C. Dodds, Experience in developing and operating integrity monitoring system in North Sea. *Proceedings of the Eighth Annual Offshore Technology Conference*, 1976, pp. 313–319.
- [5] R. Nataraja, Structural integrity monitoring in real seas. *Proceedings of the 15th Annual Offshore Technology Conference*, 1983, pp. 221–228.
- [6] T.R. Whittome, C.J. Dodds, Monitoring offshore structures by vibration techniques, *Proceedings of Design in Offshore Structures Conference*, 1983, pp. 93–100.
- [7] C.Y. Kim, N.S. Kim, D.S. Jung, J.G. Yoon, Effect of vehicle mass on the measured dynamic characteristics of bridges from traffic-induced vibration test, *Proceedings of the 19th International Modal Analysis Conference (IMAC19)*, 2001, pp. 1106–1111.
- [8] S. Roberts, Identification of the modal parameters affecting automotive ride characteristics, *Proceedings of the 19th International Modal Analysis Conference (IMAC19)*, 2001, pp. 270–274.
- [9] S.W. Doebling, C.R. Farrar, Computation of structural flexibility for bridge health monitoring using ambient modal data, *Proceedings of the 11th ASCE Engineering Mechanics Conference*, 1996, pp. 1114–1117.
- [10] R.B. Randall, Y. Gao, J. Swevers, Updating modal models from response measurements, *Proceedings of the 23rd International Conference on Noise and Vibration Engineering (ISMA23)*, 1998, pp. 1153–1160.
- [11] J. Deweer, B. Dierckx, Obtaining a scaled modal model of panel type structures using acoustic excitation, *Proceedings of the 17th International Modal Analysis Conference (IMAC17)*, 1999, pp. 2042–2048.
- [12] E. Parloo, P. Verboven, P. Guillaume, M. Van Overmeire, Sensitivity-based mass-normalization of mode shape estimates from output-only data, *Proceedings of the International Conference on Structural System Identification*, Kassel, Germany, 2001, pp. 627–636.
- [13] P. Guillaume, E. Parloo, P. Verboven, G. De Sitter, An inverse method for the identification of localized excitation sources, *Proceedings of the 20th International Modal Analysis Conference (IMAC20)*, 2002.
- [14] E. Parloo, P. Verboven, P. Guillaume, M. Van Overmeire, Sensitivity-based damage assessment technique for output-only data, *Proceedings of the Third International Workshop on Structural Health Monitoring*, Stanford, CA, 2001.
- [15] W. Heylen, S. Lammens, P. Sas, Modal analysis theory and testing, Department of Mechanical Engineering, Katholieke Universiteit Leuven, 1995.
- [16] P. Vanhonacker, Differential and difference sensitivities of natural frequencies and mode shapes of mechanical structures, *American Institute of Aeronautics and Astronautics Journal* 18 (1980) 1511–1514.
- [17] P. Vanhonacker, The Use of Modal Parameters of Mechanical Structures in Sensitivity Analysis-, System Synthesis- and System Identification Methods, PhD Thesis, Department of Mechanical Engineering, Katholieke Universiteit Leuven, 1988.
- [18] H. Van der Auweraer, W. Leurs, P. Mas, L. Hermans, Modal parameter estimation from inconsistent data sets, *Proceedings of the 18th International Modal Analysis Conference (IMAC18)*, 2000, pp. 763–771.
- [19] B. Cauberghe, P. Guillaume, B. Dierckx, Identification of modal parameters from inconsistent data, *Proceedings of the 20th International Modal Analysis Conference (IMAC20)*, 2002.
- [20] E. Parloo, P. Guillaume, M. Van Overmeire, Damage assessment using mode shape sensitivities, *Mechanical Systems & Signal Processing*, 2001, in press.
- [21] E. Parloo, P. Verboven, P. Guillaume, M. Van Overmeire, Maximum likelihood identification of modal parameters from non-stationary operational data, *Proceedings of the 19th International Modal Analysis Conference (IMAC19)*, 2001, pp. 425–431.

- [22] T. Martens, K. Wyckaert, Matrix inversion technology for vibro-acoustic modeling applications: Practical examples of measurement noise reduction by SVD, Proceedings of the 23rd International Seminar on Modal Analysis (ISMA23), September 1998, pp. 177–183.
- [23] P. Guillaume, P. Verboven, S. Vanlanduit, Frequency-domain maximum likelihood estimation of modal parameters with confidence intervals, Proceedings of the 23rd International Seminar on Modal Analysis (ISMA23), September 1998, pp. 359–366.